The Effective Theory of Inflation and keV Dark Matter in the Standard Model of the Universe

H. J. de Vega

LPTHE, CNRS/Université P & M Curie (Paris VI).

14th Paris Cosmology Colloquium 2010

Observatoire de Paris, Paris campus

Thursday 22 , Friday 23 and Saturday 24 July 2010

Standard Cosmological Model: ΛCDM

ΛCDM = Cold Dark Matter + Cosmological Constant

- Begins by the inflationary era. Slow-Roll inflation explains horizon and flatness.
- Gravity is described by Einstein's General Relativity.
- Particle Physics described by the Standard Model of Particle Physics: $SU(3) \otimes SU(2) \otimes U(1) =$ qcd+electroweak model.
- CDM: dark matter is cold (non-relativistic) during the matter dominated era where structure formation happens. DM is outside the SM of particle physics.
- Dark energy described by the cosmological constant Λ.

Standard Cosmological Model: ΛCDM

ΛCDM = Cold Dark Matter + Cosmological Constant begins by the Inflationary Era. Explains the Observations:

- Seven years WMAP data and further CMB data
- Light Elements Abundances
- Large Scale Structures (LSS) Observations. BAO.
- Acceleration of the Universe expansion: Supernova Luminosity/Distance and Radio Galaxies.
- Gravitational Lensing Observations
- Lyman α Forest Observations
- Hubble Constant (H_0) Measurements
- Properties of Clusters of Galaxies
- Measurements of the Age of the Universe

Physics during Inflation

- Out of equilibrium evolution in a fastly expanding geometry. Vacuum energy DOMINATED (De Sitter) universe $a(t) \simeq e^{H\,t}$.
- Explosive particle production due to spinodal or parametric instabilities. Quantum non-linear phenomena eventually shut-off the instabilities and stop inflation. Radiation dominated era follows: $a(t) = \sqrt{t}$.
- Huge redshift classicalizes the dynamics: an assembly of (superhorizon) quantum modes behave as a classical and homogeneous inflaton field. Inflaton slow-roll.

D. Boyanovsky, C. Destri, H. J. de Vega, N. G. Sánchez, The Effective Theory of Inflation in the Standard Model of the Universe and the CMB+LSS data analysis (review article), arXiv:0901.0549, Int.J.Mod.Phys.**A 24**, 3669-3864 (2009).

The Theory of Inflation

The inflaton is an effective field in the Ginsburg-Landau sense.

Relevant effective theories in physics:

- Ginsburg-Landau theory of superconductivity. It is an effective theory for Cooper pairs in the microscopic BCS theory of superconductivity.
- The $O(4)$ sigma model for pions, the sigma and photons at energies $\lesssim 1$ GeV. The microscopic theory is QCD: quarks and gluons. $\pi \simeq \bar{q}q$, $\sigma \simeq \bar{q}q$.
- The theory of second order phase transitions à la Landau-Kadanoff-Wilson... (ferromagnetic, antiferromagnetic, liquid-gas, Helium 3 and 4, ...)
- Fermi Theory of Weak Interactions (current-current).

Slow Roll Inflation

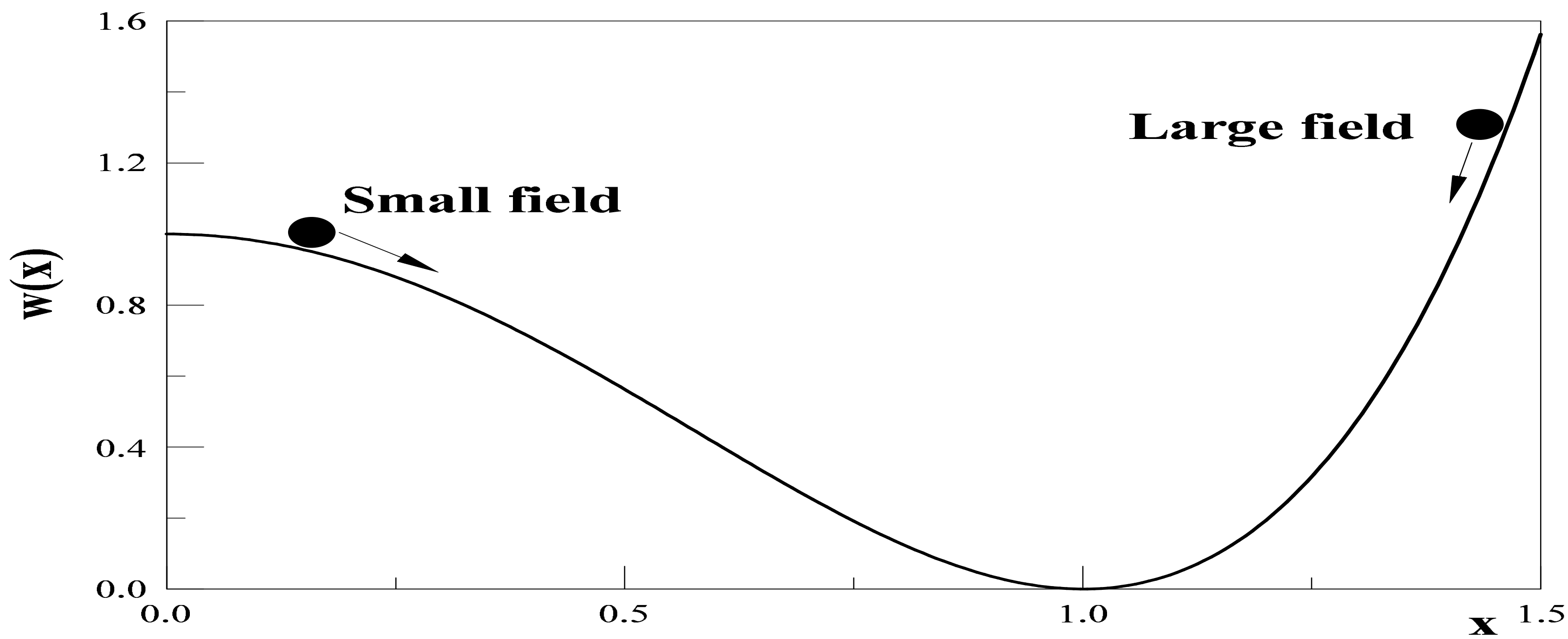

The field evolves towards the minimum of the potential.

$V(\mathrm{Min}) = V'(\mathrm{Min}) = 0$: inflation ends after a finite number of efolds. Slow-roll is needed to produce enough efolds of inflation (≥ 62) to explain the part of todays's entropy in the universe having a primordial origin.

$\Longrightarrow$ the slope of the potential $V(\phi)$ must be small.

Effective Theory of Inflation: à la Ginsburg-Landau

N efolds since the inflaton exits the horizon till the end of inflation: $N \sim 60$.
In the effective theory of inflation the slow-roll inflaton potential has the universal form:

$V(\phi) = N\ M^4\ w(\chi)\ ,\ M =$ energy scale of inflation,
$\chi \equiv \frac{\phi}{\sqrt{N}\ M_{Pl}} =$ dimensionless and slow field.
$\chi = \mathcal{O}(1)\ ,\ w(\chi) = \mathcal{O}(1)$

We find in this effective theory of inflation for the adiabatic Scalar Perturbations: $P(k) = |\Delta_{k\ ad}^{(S)}|^2\ k^{n_s-1}$:

$$|\Delta_{k\ ad}^{(S)}|^2 = \frac{N^2}{12\,\pi^2}\ \left(\frac{M}{M_{Pl}}\right)^4\ \frac{w^3(\chi)}{w'^2(\chi)} \sim \frac{N^2}{12\,\pi^2}\ \left(\frac{M}{M_{Pl}}\right)^4\ .$$

for all slow-roll inflation models:
The WMAP7 result: $|\Delta_{k\ ad}^{(S)}| = (0.494 \pm 0.01) \times 10^{-4}$
determines the scale of inflation M (using $N \simeq 60$).

Inflation energy scale M, the spectral index n_s and the ratio

$(M/M_{Pl})^2 = 0.85 \times 10^{-5} \longrightarrow M = 0.70 \times 10^{16}$ GeV

The inflation energy scale M turns to be
the grand unification energy scale !!

The scale M is independent of the shape of $w(\chi)$.

We find the scale of inflation without knowing the ratio r of tensor to scalar fluctuations.
(tensor fluctuations = primordial gravitons).

$$n_s - 1 = -\frac{3}{N}\left[\frac{w'(\chi)}{w(\chi)}\right]^2 + \frac{2}{N}\,\frac{w''(\chi)}{w(\chi)} \quad , \quad r = \frac{8}{N}\left[\frac{w'(\chi)}{w(\chi)}\right]^2$$

χ is the inflaton field at horizon exit.

We obtain the model independent estimates:

$n_s - 1$ and r are of the order $1/N \sim 0.02$,

$dn_s/d\ln k$ is of the order $1/N^2 \sim 0.0003 \Leftarrow$ negligible !!

MCMC Results for the double–well inflaton potential

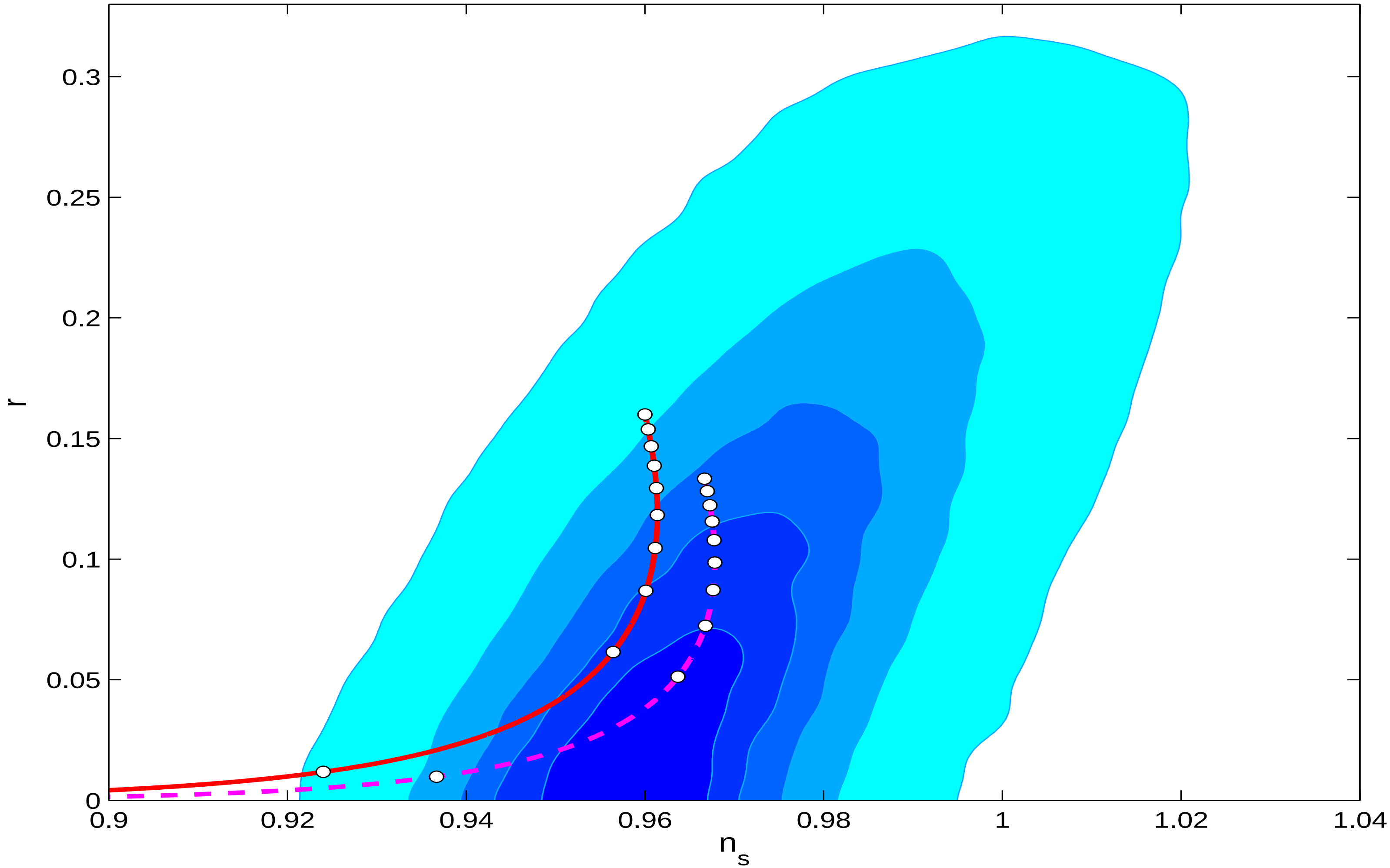

Solid line for $N = 50$ and dashed line for $N = 60$
White dots: $z = 0.01 + 0.11 * n, \ n = 0, 1, \ldots, 9$,
y increases from the uppermost dot $y = 0, \ z = 1$.

MCMC Results for double–well inflaton potential

Bounds: $r > 0.023$ (95% CL) , $r > 0.046$ (68% CL)
Most probable values: $n_s \simeq 0.964$, $r \simeq 0.051 \Leftarrow$measurable!!
The most probable double–well inflaton potential has a moderate nonlinearity with the quartic coupling $y \simeq 1.26 \ldots$.
The $\chi \to -\chi$ symmetry is here spontaneously broken since the absolute minimum of the potential is at $\chi \neq 0$

$$w(\chi) = \frac{y}{32}\left(\chi^2 - \frac{8}{y}\right)^2$$

MCMC analysis calls for $w''(\chi) < 0$ at horizon exit
$\Longrightarrow$ double well potential favoured.
C. Destri, H. J. de Vega, N. Sanchez, Phys. Rev. D77, 043509 (2008), astro-ph/0703417.

Planck may measure such $r \simeq 0.05$: borderline
C. Burigana, C. Destri, H. J. de Vega, A. Gruppuso, N. Mandolesi, P. Natoli, N. G. Sanchez, arXiv:1003.6108.

Quantum Fluctuations During Inflation and after

The Universe is homogeneous and isotropic after inflation thanks to the fast and gigantic expansion stretching lenghts by a factor $e^{62} \simeq 10^{27}$. By the end of inflation: $T \sim 10^{14}$ GeV.

Quantum fluctuations around the classical inflaton and FRW geometry were of course present.

These inflationary quantum fluctuations are the seeds of the structure formation and of the CMB anisotropies today: galaxies, clusters, stars, planets, ...

That is, our present universe was built out of inflationary quantum fluctuations. CMB anisotropies spectrum:

$3 \times 10^{-32}\text{cm} < \lambda_{begin\,inflation} < 3 \times 10^{-28}\text{cm}$

$M_{Planck} \gtrsim 10^{18}$ GeV $> \lambda^{-1}_{begin\,inflation} > 10^{14}$ GeV.

total redshift since inflation begins till today $= 10^{56}$:

0.1 Mpc $< \lambda_{today} <$ 1 Gpc , 1 pc = 3×10^{18} cm $= 200000$ AU

Universe expansion classicalizes the physics: decoherence

Dark Matter

DM particles can decouple being ultrarelativistic (UR) at $T_d \gg m$ or non-relativistic $T_d \ll m$.

We consider particles that decouple at or out of LTE (LTE = local thermal equilibrium).

Distribution function: $F_d[p_c]$ freezes out at decoupling.

$p_c =$ comoving momentum.

$P_f(t) = p_c/a(t) =$ Physical momentum,

Velocity fluctuations: $y = P_f(t)/T_d(t) = p_c/T_d$

$$\langle \vec{V}^2(t) \rangle = \langle \frac{\vec{P}_f^2(t)}{m^2} \rangle = \left[\frac{T_d}{m \; a(t)} \right]^2 \; \frac{\int_0^\infty y^4 F_d(y) dy}{\int_0^\infty y^2 F_d(y) dy} \; .$$

Energy Density: $\rho_{DM}(t) = \frac{m \; g}{2\pi^2} \; \frac{T_d^3}{a^3(t)} \int_0^\infty y^2 \; F_d(y) \; dy$,

g : $\#$ of internal degrees of freedom of the DM particle, $1 \leq g \leq 4$. Formula valid when DM particles are non-relativistic.

Dark Matter density and DM velocity dispersion

Using entropy conservation: $T_d = \left(\frac{2}{g_d}\right)^{\frac{1}{3}} \; T_{cmb}$,

$g_d =$ effective $\#$ of UR degrees of freedom at decoupling,

$T_{cmb} = 0.2348 \; 10^{-3}$ eV, and

$\rho_{DM}(\text{today}) = \frac{m \; g}{\pi^2 \; g_d} \; T_{cmb}^3 \int_0^\infty y^2 \; F_d(y) \; dy = 1.107 \; \frac{\text{keV}}{\text{cm}^3}$ (1)

We obtain for the primordial velocity dispersion:

$$\sigma_{prim}(z) = \sqrt{\frac{1}{3} \; \langle \vec{V}^2 \rangle(z)} = 0.05124 \; \frac{1+z}{g_d^{\frac{1}{3}}} \left[\frac{\int_0^\infty y^4 \; F_d(y) \; dy}{\int_0^\infty y^2 \; F_d(y) \; dy}\right]^{\frac{1}{2}} \frac{\text{keV}}{m} \, \frac{\text{km}}{\text{s}}$$

Goal: determine m and g_d. We need TWO constraints.

Notice that $F_d(y)$ and $I_{2n} = \int_0^\infty y^{2n} \; F_d(y) \; dy \quad , \quad n = 1, 2.$

are quantities of order one.

The Phase-space density $Q = \rho/\sigma^3$ and its decrease factor Z

The phase-space density $Q \equiv \rho/\sigma^3$ is invariant under the cosmological expansion and can only decrease under self-gravity interactions (gravitational clustering).

The phase-space density today follows observing dwarf spheroidal satellite galaxies of the Milky Way (dSphs)

$\frac{\rho_s}{\sigma_s^3} \sim 5 \times 10^3 \, \frac{\text{keV/cm}^3}{(\text{km/s})^3} = (0.18 \text{ keV})^4$ Gilmore et al. 07 and 08.

During structure formation $(z \lesssim 30)$, $Q = \rho/\sigma^3$ decreases by a factor that we call Z:

$$Q_{today} = \frac{1}{Z}\, Q_{prim} \quad , \quad Q_{prim} = \frac{\rho_{prim}}{\sigma^3_{prim}} \quad , \qquad (2) \qquad Z > 1.$$

The spherical model gives $Z \simeq 41000$ and N-body simulations indicate: $10000 > Z > 1$. Z is galaxy dependent.

Constraints: First $\rho_{DM}(\text{today})$, Second $Q_{today} = \rho_s/\sigma_s^3$

Mass Estimates for DM particles

Combining the previous expressions lead to general formulas for m and g_d:

$$m = \frac{2^{\frac{1}{4}}\sqrt{\pi}}{3^{\frac{3}{8}}\, g^{\frac{1}{4}}}\, Q_{prim}^{\frac{1}{4}}\, I_4^{\frac{3}{8}}\, I_2^{-\frac{5}{8}} \; , \quad g_d = \frac{2^{\frac{1}{4}}\, g^{\frac{3}{4}}}{3^{\frac{3}{8}}\, \pi^{\frac{3}{2}}\, \Omega_{DM}}\; \frac{T_\gamma^3}{\rho_c}\, Q_{prim}^{\frac{1}{4}}\, [I_2\, I_4]^{\frac{3}{8}}$$

where: $Q_{prim}^{\frac{1}{4}} = Z^{\frac{1}{4}}\; 0.18$ keV using the dSphs data,

$T_\gamma = 0.2348 \text{ meV}\; , \; \Omega_{DM} = 0.228 \; , \; \rho_c = (2.518 \text{ meV})^4$

$I_{2\,n} = \int_0^\infty y^{2\,n}\, F_d(y)\, dy \quad , \quad n = 1, 2.$

These formulas yield for relics decoupling UR at LTE:

$$m = \left(\frac{Z}{g}\right)^{\frac{1}{4}} \text{keV} \left\{ \begin{array}{c} 0.568 \\ 0.484 \end{array} \right. , \; g_d = g^{\frac{3}{4}}\, Z^{\frac{1}{4}} \left\{ \begin{array}{ll} 155 & \text{Fermions} \\ 180 & \text{Bosons} \end{array} \right. .$$

Since $g = 1 - 4$, we see that $g_d \gtrsim 100 \Rightarrow T_d \gtrsim 100$ GeV.

$1 < Z^{\frac{1}{4}} < 10$ for $1 < Z < 10000$. Example: for DM Majorana fermions $(g = 2)$ $m \simeq 0.85$ keV.

Out of thermal equilibrium decoupling

Results for m and g_d on the same scales for DM particles decoupling UR out of thermal equilibrium.

For a specific model of sterile neutrinos where decoupling is out of thermal equilibrium:

$$0.56 \text{ keV} \lesssim m_\nu \, Z^{-\frac{1}{4}} \lesssim 1.0 \text{ keV} \quad , \quad 15 \lesssim g_d \, Z^{-\frac{1}{4}} \lesssim 84$$

Relics decoupling non-relativistic:
similar bounds: keV $\lesssim m \lesssim$ MeV

D. Boyanovsky, H. J. de Vega, N. Sanchez,
Phys. Rev. D 77, 043518 (2008), arXiv:0710.5180.

H. J. de Vega, N. G. Sanchez, MNRAS 404, 885 (2010),
arXiv:0901.0922.

Linear primordial power today $P(k)$ vs. k Mpc h

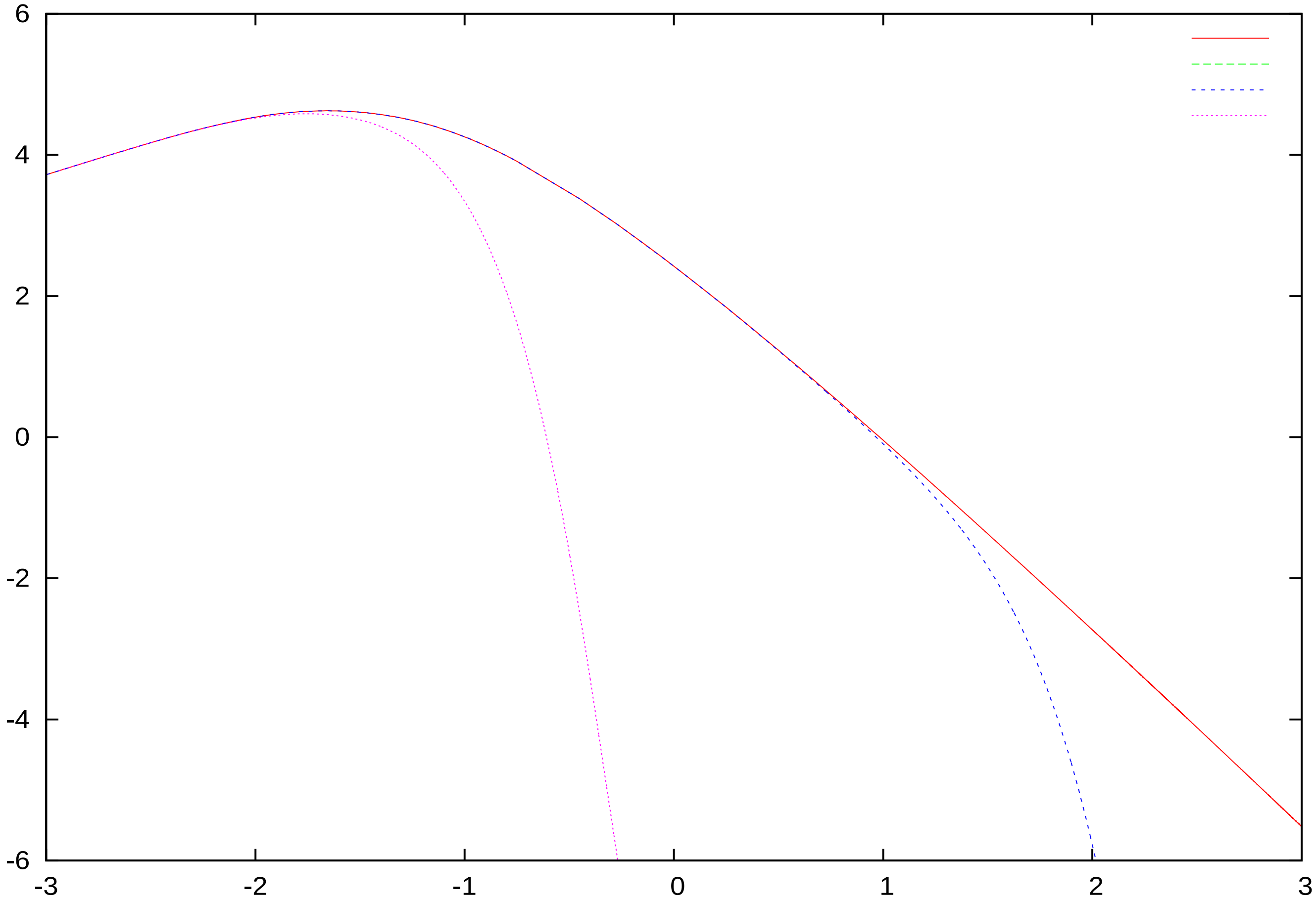

$\log_{10} P(k)$ vs. $\log_{10}[k \text{ Mpc } h]$ for WIMPS, 1 keV DM particles and 10 eV DM particles. $P(k) = P_0 \, k^{n_s} \, T^2(k)$.

$P(k)$ cutted for 1 keV DM particles on scales $\lesssim 100$ kpc.

Transfer function in the MD era from Gilbert integral eq

Galaxies

Physical variables in galaxies:

a) Nonuniversal quantities: mass, size, luminosity, fraction of DM, DM core radius r_0, central DM density ρ_0, ...

b) Universal quantities: surface density $\mu_0 \equiv r_0 \, \rho_0$ and DM density profiles. M_{BH}/M_{halo} (or the halo binding energy).

The galaxy variables are related by universal empirical relations. Only one variable remains free.

Universal quantities may be attractors in the dynamical evolution.

Universal DM density profile in Galaxies:

$$\rho(r) = \rho_0 \, F\left(\frac{r}{r_0}\right) \ , \ F(0) = 1 \ , \ x \equiv \frac{r}{r_0} \ , \ r_0 = \text{DM core radius.}$$

Empirical cored profiles: $F_{Burkert}(x) = \frac{1}{(1+x)(1+x^2)}$.

Cored profiles do reproduce the astronomical observations.

The constant surface density in DM and luminous galaxies

The Surface density for dark matter (DM) halos and for luminous matter galaxies defined as: $\mu_{0D} \equiv r_0 \; \rho_0$,

$r_0 =$ halo core radius, $\rho_0 =$ central density for DM galaxies

$\mu_{0D} \simeq 120 \; \frac{M_\odot}{\mathrm{pc}^2} = 5500 \; (\mathrm{MeV})^3 = (17.6 \; \mathrm{Mev})^3$

5 kpc < r_0 < 100 kpc. For luminous galaxies $\rho_0 = \rho(r_0)$. Donato et al. 09, Gentile et al. 09

Universal value for μ_{0D}: independent of galaxy luminosity for a large number of galactic systems (spirals, dwarf irregular and spheroidals, elliptics) spanning over 14 magnitudes in luminosity and of different Hubble types.

Similar values $\mu_{0D} \simeq 80 \; \frac{M_\odot}{\mathrm{pc}^2}$ in interstellar molecular clouds of size r_0 of different type and composition over scales $0.001 \, \mathrm{pc} < r_0 < 100$ pc (Larson laws, 1981).

Scaling of the energy and entropy from the surface density

Total energy using the virial and the profile $F(x)$:

$$E = \frac{1}{2}\,\langle U \rangle = -\frac{1}{4}\,G\,\int \frac{d^3r\,d^3r'}{|\boldsymbol{r}-\boldsymbol{r}'|}\,\langle \rho(r)\,\rho(r')\rangle =$$

$$= -\frac{1}{4}\,G\,\rho_0^2\,r_0^5 \int \frac{d^3x\,d^3x'}{|\boldsymbol{x}-\boldsymbol{x}'|}\,\langle F(x)\,F(x')\rangle \quad \Rightarrow \quad E \sim G\,\mu_{0D}^2\,r_0^3$$

The energy scales as the volume.

For consistency with the profile, the Boltzmann-Vlasov distribution function must scale as

$$f(\boldsymbol{p},\boldsymbol{r}) = \frac{1}{m^4\,r_0^3\,G^{\frac{3}{2}}\,\sqrt{\rho_0}}\,\mathcal{F}\left(\frac{\boldsymbol{p}}{m\,r_0\,\sqrt{G\,\rho_0}},\frac{\boldsymbol{r}}{r_0}\right)$$

Hence, the entropy scales as

$$S = \int f(\boldsymbol{p},\boldsymbol{r})\,\log f(\boldsymbol{p},\boldsymbol{r})\,d^3p\,d^3r \sim r_0^3\,\frac{\rho_0}{m} = r_0^2\,\frac{\mu_{0D}}{m}\;.$$

The entropy scales as the surface (as for black-holes). However, very different proportionality coefficients: $\frac{S_{BH}/A}{S_{gal}/r_0^2} \sim \frac{m}{\mathrm{keV}}\,10^{36} \Rightarrow$ Much smaller coefficient for galaxies than for black-holes. Bekenstein bound satisfied.

DM surface density from linear Boltzmann-Vlasov eq

The distribution function of the decoupled DM particles:

$$f(\vec{x}, \vec{p}; t) = g\ f_0(p) + F_1(\vec{x}, \vec{p}; t)$$

$f_0(p) =$ thermal equilibrium function at temperature T_d.

We evolve the distribution function $F_1(\vec{x}, \vec{p}; t)$ according to the linearized Boltzmann-Vlasov equation since the end of inflation where the primordial inflationary fluctuations are:

$$|\phi_k| = \sqrt{2}\ \pi\ \frac{|\Delta_0|}{k^{\frac{3}{2}}}\ \left(\frac{k}{k_0}\right)^{\frac{n_s-1}{2}}$$ where

$$|\Delta_0| \simeq 4.94\ 10^{-5},\ n_s \simeq 0.964,\ k_0 = 2\ \mathrm{Gpc}^{-1}.$$

We Fourier transform over $\vec{x}$ and integrate over momentum

$$\Delta(k, t) \equiv m\ \int \frac{d^3p}{(2\pi)^3}\ \int d^3x\ e^{-i\,\vec{x}\cdot\vec{k}}\ F_1(\vec{x}, \vec{p}; t)$$

The matter density fluctuations $\rho_{lin}(r)$ are given today by

$$\rho_{lin}(r) = \frac{1}{2\,\pi^2\,r}\ \int_0^\infty k\ dk\ \sin(k\,r)\ \Delta(k, t_{\mathrm{today}})$$

Linear density fluctuations today

$\Delta(k,z) \stackrel{z\to 0}{=} \frac{3}{5}\, T(k)\, (1+z_{eq})\, \Delta(k,z_{eq}) \quad , \quad {}_{eq} =$ equilibration,

$T(k) =$ transfer function during the matter dominated era

$T(0) = 1 \quad , \quad T(k \to \infty) = 0$ and $1 + z_{eq} \simeq 3200$.

$T(k)$ decreases with k with the characteristic free streaming scale $k_{fs} = \sqrt{2}/r_{lin}$,

$$r_{lin} = 2\,\sqrt{1+z_{eq}}\,\left(\frac{3\,M_{Pl}^2}{H_0\,\sqrt{\Omega_{DM}}\,Q_{prim}}\right)^{\frac{1}{3}}$$ and $\gamma \equiv k\, r_{lin}$.

The linear profile today results:

$$\rho_{lin}(r) = \frac{27\,\sqrt{2}}{5\,\pi}\,\frac{\Omega_M^2\,M_{Pl}^2\,H_0}{\sigma_{DM}^2}\,b_0\,b_1\,9.6\,|\Delta_0|\,\left(k_{eq}\,r_{lin}\right)^{\frac{3}{2}} \times$$
$$\left(k_0\,r_{lin}\right)^{\frac{1-n_s}{2}}\,\frac{1}{r}\,\int_0^\infty d\gamma\,N(\gamma)\,\sin\left(\gamma\,\frac{r}{r_{lin}}\right)$$

where $N(\gamma) \equiv \gamma^{n_s/2-1}\,\log\left(\frac{c\,\gamma}{k_{eq}\,r_{lin}}\right)\,T(\gamma) \quad , \quad c \simeq 0.11604$.

Transfer function $T(k)$

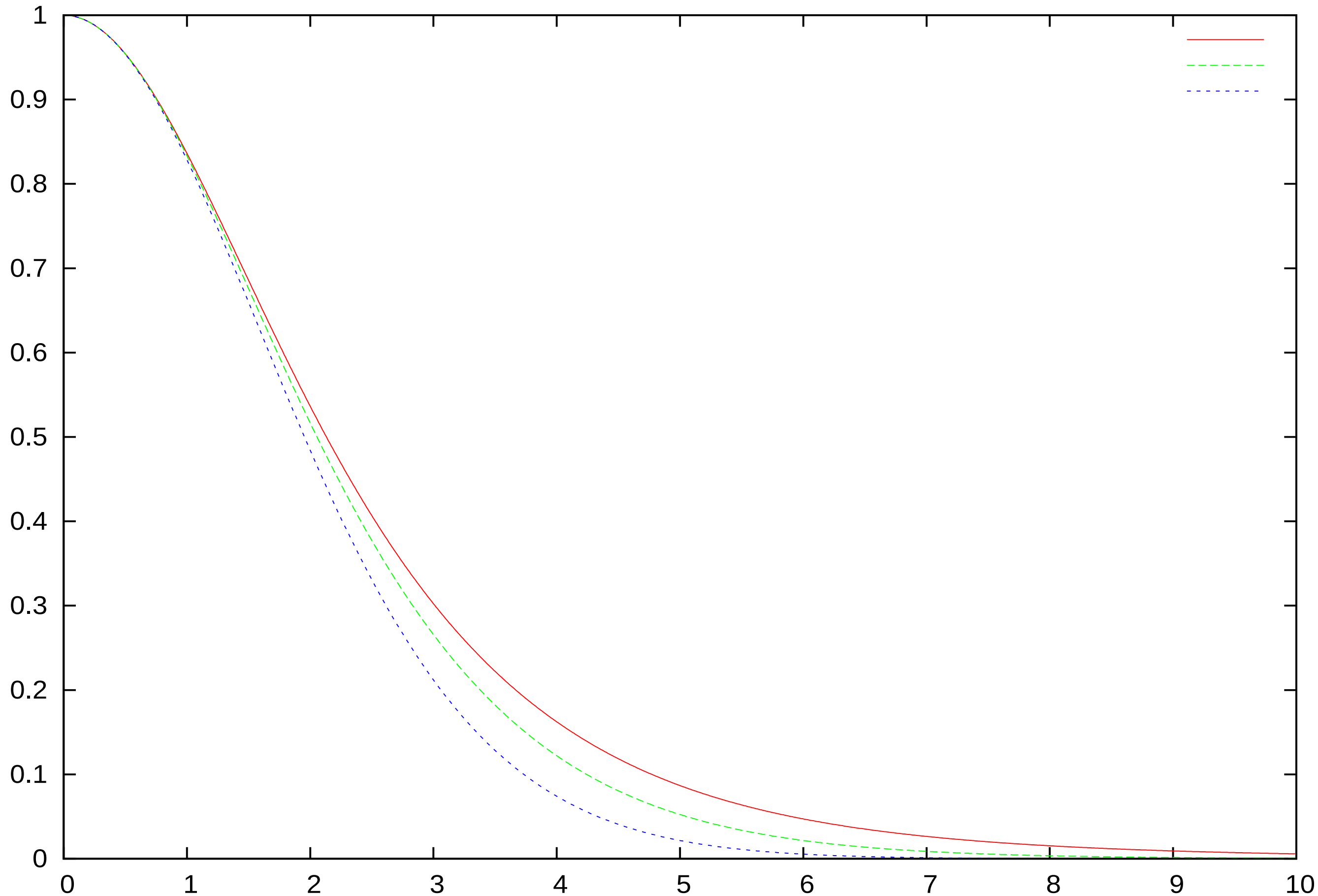

$T(k)$ vs. $\gamma = k\, r_{lin}$ for Fermions and Bosons decoupling ultrarelativistically and for particles decoupling non-relativistically (Maxwell-Boltzmann statistics).

Density profiles in the linear approximation

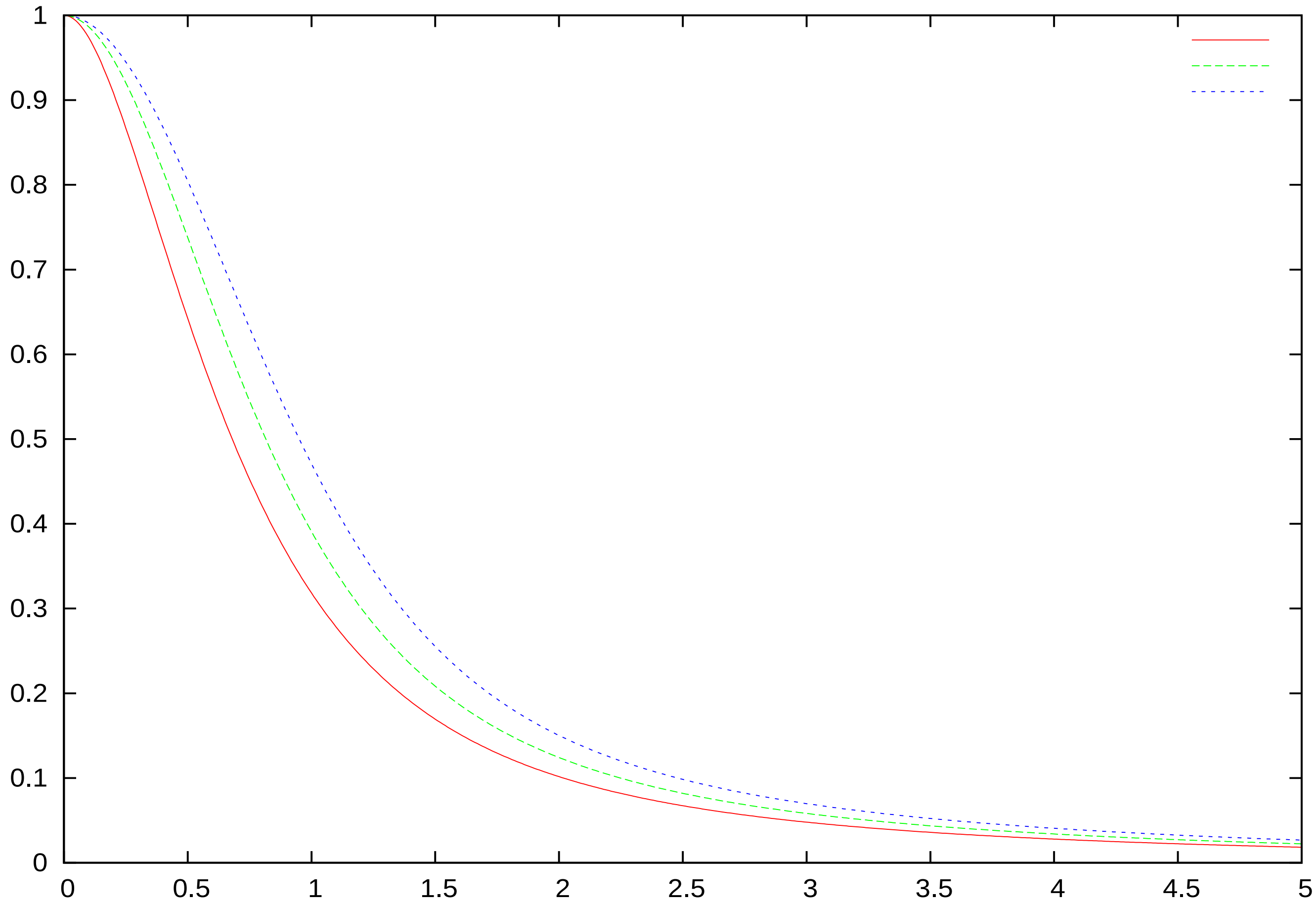

Profiles $\rho_{lin}(r)/\rho_{lin}(0)$ vs. $x \equiv r/r_{lin}$. These are universal profiles as functions of x. r_{lin} depends on the galaxy.

Fermions and Bosons decoupling ultrarelativistically and particles decoupling non-relativistically (Maxwell-Boltzmann statistics)

Matching the observed and the theoretical surface density

Surface density: $\mu_0 \equiv r_0 \, \rho(0)$ where $r_0 =$ core radius.

Linear approximation: $r_{lin} = \alpha \, r_0$. α follows fitting the linear profile $\rho_{lin}(r)$ to the Burkert profile with core radius r_0.

$\alpha-$values: $\alpha_{BE} = 0.805 \, , \alpha_{FD} = 0.688 \, , \alpha_{MB} = 0.421$.

Theoretical result: $\mu_{0\,lin} = r_{lin} \, \rho_{lin}(0)/\alpha$.

Fermions:

$$\mu_{0\,lin} = 8261 \, \left[\frac{Q_{prim}}{(\mathrm{keV})^4}\right]^{0.161} \left[1 + 0.0489 \, \ln \frac{Q_{prim}}{(\mathrm{keV})^4}\right] \mathrm{MeV}^3$$

Here: $0.161 = n_s/6$.

Matching the observed values $\mu_{0\,obs}$ with this $\mu_{0\,lin}$ gives $Q_{prim}/(\mathrm{keV})^4$ and the mass of the DM particle as

$m = m_0 \, Q_{prim}^{\frac{1}{4}}/\mathrm{keV}$, data from spiral galaxies.

BE: $m_0 = 2.6462$ keV, FD: $m_0 = 2.6934$ keV.

$Q_{prim}/(\mathrm{keV})^4$ from the observed surface density

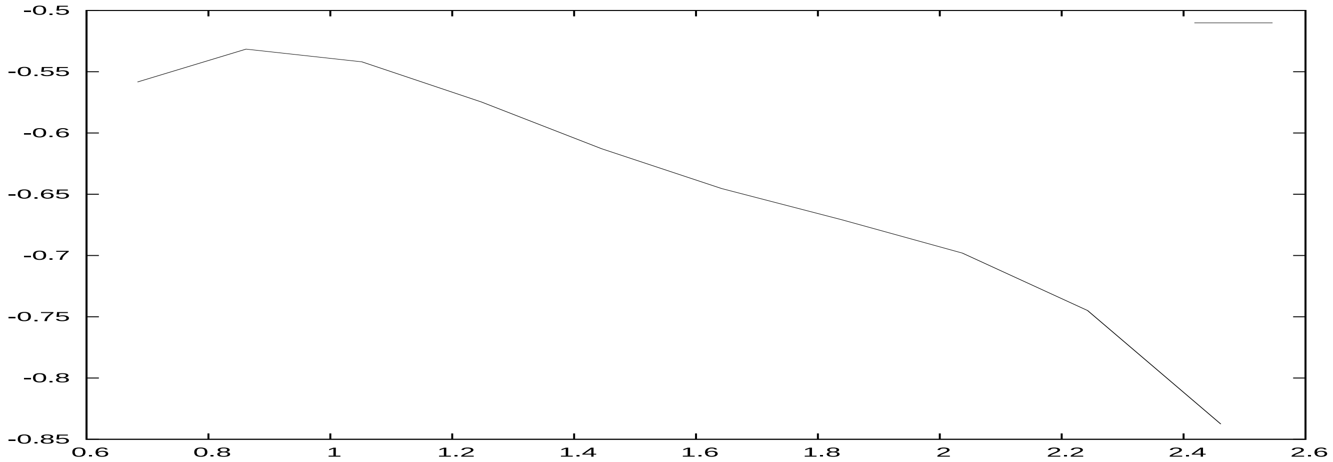

$\log_{10} Q_{prim}/(\mathrm{keV})^4$ vs. $\log_{10} M_{virial}/[10^{11} M_\odot]$

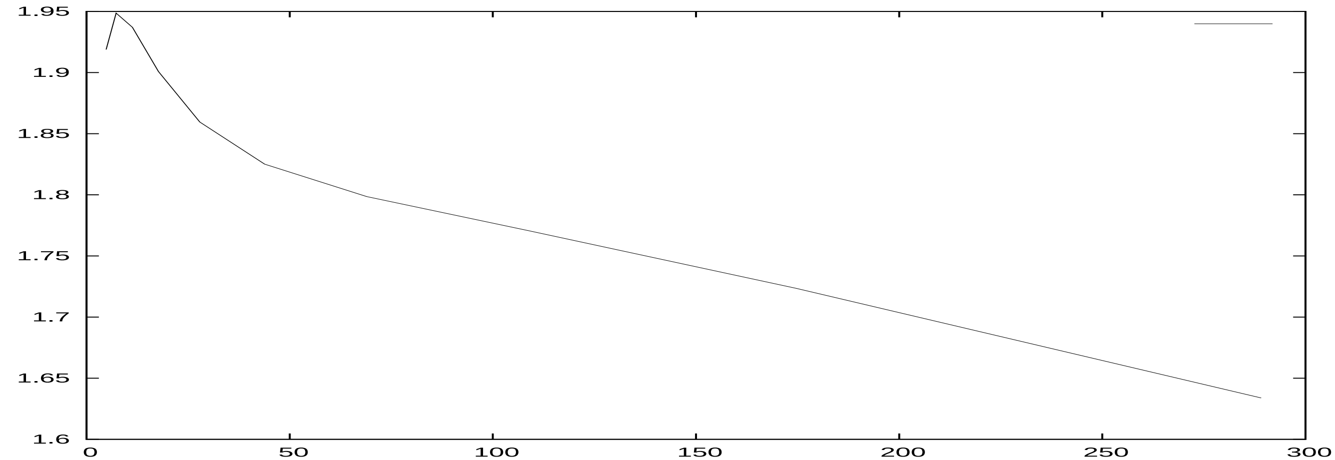

m in keV vs. $M_{virial}/[10^{11} M_\odot]$

Density profiles in the linear approximation

Density profiles turn to be cored at scales $r \ll r_{lin}$.

Intermediate regime $r \gtrsim r_{lin}$:

$$\rho_{lin}(r) \overset{r \gtrsim r_{lin}}{=} \left(\frac{36.45 \text{ kpc}}{r}\right)^{1+n_s/2} \ln\left(\frac{7.932 \text{ Mpc}}{r}\right) \times$$
$$\left[1 + 0.2416 \ \ln\left(\frac{m}{\text{keV}}\right)\right] \ 10^{-26} \ \frac{\text{g}}{\text{cm}^3} \quad , \quad 1 + n_s/2 = 1.482.$$

$\rho_{lin}(r)$ scales with the primordial spectral index n_s.

The theoretical linear results agree with the universal empirical behaviour $r^{-1.6 \pm 0.4}$: M. G. Walker et al. (2009) (observations), I. M. Vass et al. (2009) (simulations).

The agreement between the linear theory and the observations is remarkable.

Non-universal galaxy properties.

	Observed Values	Linear Theory
r_0	5 to 52 kpc	46 to 59 kpc
ρ_0	1.57 to $19.3 \times 10^{-25}\ \frac{\mathrm{g}}{\mathrm{cm}^3}$	1.49 to $1.91 \times 10^{-25}\ \frac{\mathrm{g}}{\mathrm{cm}^3}$
$\sqrt{\overline{v^2}}_{halo}$	79.3 to 261 km/sec	260 km/sec

Dark matter particle mass: $1.6 < m < 2$ keV.

The larger and less denser are the galaxies, the better are the results from the linear theory for non-universal quantities.

The linear approximation turns to improve for larger galaxies (i. e. more diluted).

Therefore, universal quantities can be reproduced by the linear approximation.

Wimps vs. galaxy observations

	Observed Values	Wimps in linear theory
r_0	5 to 52 kpc	0.045 pc
ρ_0	1.57 to $19.3 \times 10^{-25}\ \frac{\mathrm{g}}{\mathrm{cm}^3}$	$0.73 \times 10^{-14}\ \frac{\mathrm{g}}{\mathrm{cm}^3}$
$\sqrt{\overline{v^2}}_{halo}$	79.3 to 261 km/sec	0.243 km/sec

The wimps values strongly disagree by several order of magnitude with the observations. (Here $m_{wimp} = 100$ GeV).

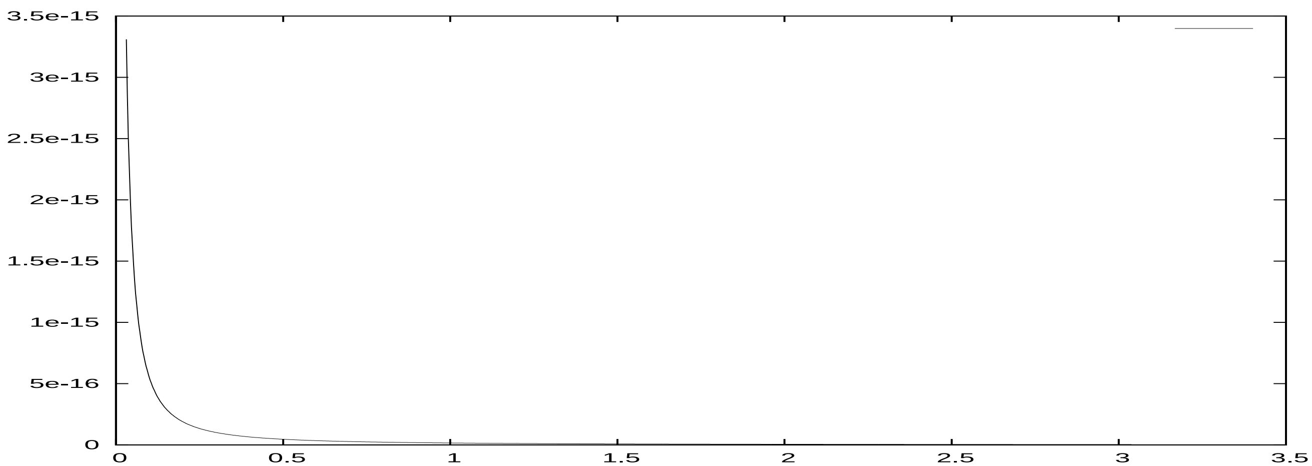

$\rho_{lin}(r)_{wimp}$ in g/cm^3 vs. r in pc. Exhibits a cusp behaviour for $r \gtrsim 0.03$ pc.

Particle physics candidates for DM

No particle in the Standard Model of particle physics (SM) can play the role of DM.

Many extensions of the SM can be envisaged to include a DM particle with mass in the keV scale and weakly enough coupled to the Standard Model particles to fulfill all particle physics experimental constraints.

Main candidates in the keV mass scale: sterile neutrinos, gravitinos, light neutralino, majoron ...

Particle physics motivations for sterile neutrinos:

There are both left and right handed quarks (with respect to the chirality).

It is natural to have right handed neutrinos ν_R besides the known left-handed neutrino. Quark-lepton similarity.

Sterile Neutrinos in the SM of particle physics

SM symmetry group: $SU(3)_{color} \otimes SU(2)_{weak} \otimes U(1)_{hypercharge}$

Leptons are color singlets and doublets under weak SU(2).

Sterile neutrinos ν_R do not participate to weak interactions.
Hence, they must be singlets of color, weak SU(2) and hypercharge.

Mixing (bilinear) terms appear: $\bar\nu_R \, \nu_L$ and $\bar\nu_L \, \nu_R$.
They produce transmutations $\nu_L \Leftrightarrow \nu_R$.

Neutrino mass matrix: $(\bar\nu_L \; \bar\nu_R) \begin{pmatrix} 0 & m_D \\ m_D & M \end{pmatrix} \begin{pmatrix} \nu_L \\ \nu_R \end{pmatrix}$

Seesaw mass eigenvalues: $\frac{m_D^2}{M}$ and M, with eigenvectors:

- active neutrino: $\nu_{active} \simeq \nu_L - \frac{m_D}{M} \, \nu_R, \quad M \gg m_D$.
- sterile neutrino: $\nu_{sterile} \simeq \nu_R + \frac{m_D}{M} \, \nu_L, \quad M \gg m_D^2/M$.

Sterile Neutrinos

Choosing $M \sim 1$ keV and $m_D \sim 0.1$ eV is consistent with observations.

Mixing angle: $\theta \sim \frac{m_D}{M} \sim 10^{-4}$ is appropriate to produce enough sterile neutrinos accounting for the observed DM.

Smallness of θ makes very difficult detection of steriles.

Precise measure of nucleus recoil in tritium beta decay: ${}^3H_1 \Longrightarrow {}^3He_2 + e^- + \bar{\nu}$ can show the presence of a sterile instead of the active $\bar{\nu}$ in the decay products.

Rhenium 187 beta decay gives $\theta < 0.009$ for 1 keV steriles [Galeazzi et al. PRL, 86, 1978 (2001)].
Available energy: $Q({}^{187}Re) = 2.47$ keV, $Q({}^3H_1) = 18.6$ keV.

Conclusion: the empty slot of right-handed neutrinos in the Standard Model of particle physics can be filled by keV-scale sterile neutrinos describing the DM.

Summary: keV scale DM particles

- Reproduce the phase-space density observed in dwarf satellite galaxies and spiral galaxies (dV S 2009).
- Provide cored universal galaxy profiles in agreement with observations (dV S 2009,dV S S 2010). (Review on cores vs. cusps by de Blok 2010, Salucci & Frigerio Martins 2009)
- Reproduce the universal surface density μ_0 of DM dominated galaxies (dV S S 2010). WIMPS simulations give 10^9 times the observed value of μ_0 (Hoffman et al. 2007).
- Alleviate the satellite problem which appears when wimps are used (Avila-Reese et al. 2000, Götz & Sommer-Larsen 2002)
- Alleviate the voids problem which appears when wimps are used (Tikhonov et al. 2009).

Summary: keV scale DM particles

- All direct searches of DM particles look for $m \gtrsim 1$ GeV. DM mass in the keV scale explains why nothing has been found ...
  e^+ and $\bar{p}$ excess in cosmic rays may be explained by astrophysics: P. L. Biermann et al. (2009), P. Blasi, P. D. Serpico (2009).
- Peculiar velocities in galaxy clusters. Wimp simulations give velocities below observations by factors $4-10$ (Kashlinsky et al. 2008, Watkins et al. 2009, Lee & Komatsu 2010). keV scale DM should alleviate this.
- Galaxies from Wimps simulations are too small (Ryan Joung et al. 2009, Holz & Perlmutter 2010). keV scale DM may alleviate this problem.

Reliable simulations with keV mass DM are needed to clarify all these issues.

Summary and Conclusions

- Combining theoretical evolution of fluctuations through the Boltzmann-Vlasov equation with galaxy data points to a DM particle mass 1 - 2 keV. T_d may be > 100 GeV. This is independent of the DM particle physics model.
- Universal Surface density in DM galaxies [$\mu_{0D} \simeq (18 \text{ MeV})^3$] explained by keV mass scale DM. Density profile scales and decreases for intermediate scales with the spectral index $n_s : \ \rho(r) \sim r^{-1-n_s/2}$.

H. J. de Vega, P. Salucci, N. G. Sanchez, 'Universal galaxy properties and the mass of the dark matter particle from theory and observations: the power of the linear approximation', arXiv:1004.1908.
H. de Vega, N. Sanchez, 'Constant surface density in dark matter galaxies', arXiv:0907.0006 and 'Model independent analysis of dark matter points to a particle mass at the keV scale', arXiv:0901.0922, MNRAS 404, 885 (2010).

Future Perspectives

The Golden Age of Cosmology and Astrophysics continues.

Galaxy and Star formation. DM properties from galaxy observations. Better upper bounds on DM cross-sections.

DM in planets and the earth. Flyby and Pioneer anomalies?

Chandra, Suzaku X-ray data: keV mass DM decay?

Sun models well reproduce the sun's chemical composition but not the heliosismology (Asplund et al. 2009).
Can DM inside the Sun help to explain the discrepancy?

Nature of Dark Matter? 83% of the matter in the universe.

Light DM particles are strongly favoured $m_{DM} \sim$ keV.
Sterile neutrinos ? Other particle in the keV mass scale?

Precision determination of DM properties (mass, T_d, nature) from better galaxy data combined with theory (Boltzmann-Vlasov and simulations).

The Universe is our ultimate physics laboratory

THANK YOU VERY MUCH

FOR YOUR ATTENTION!!

ρ/σ^3 vs. r for different z from ΛCDM simulations

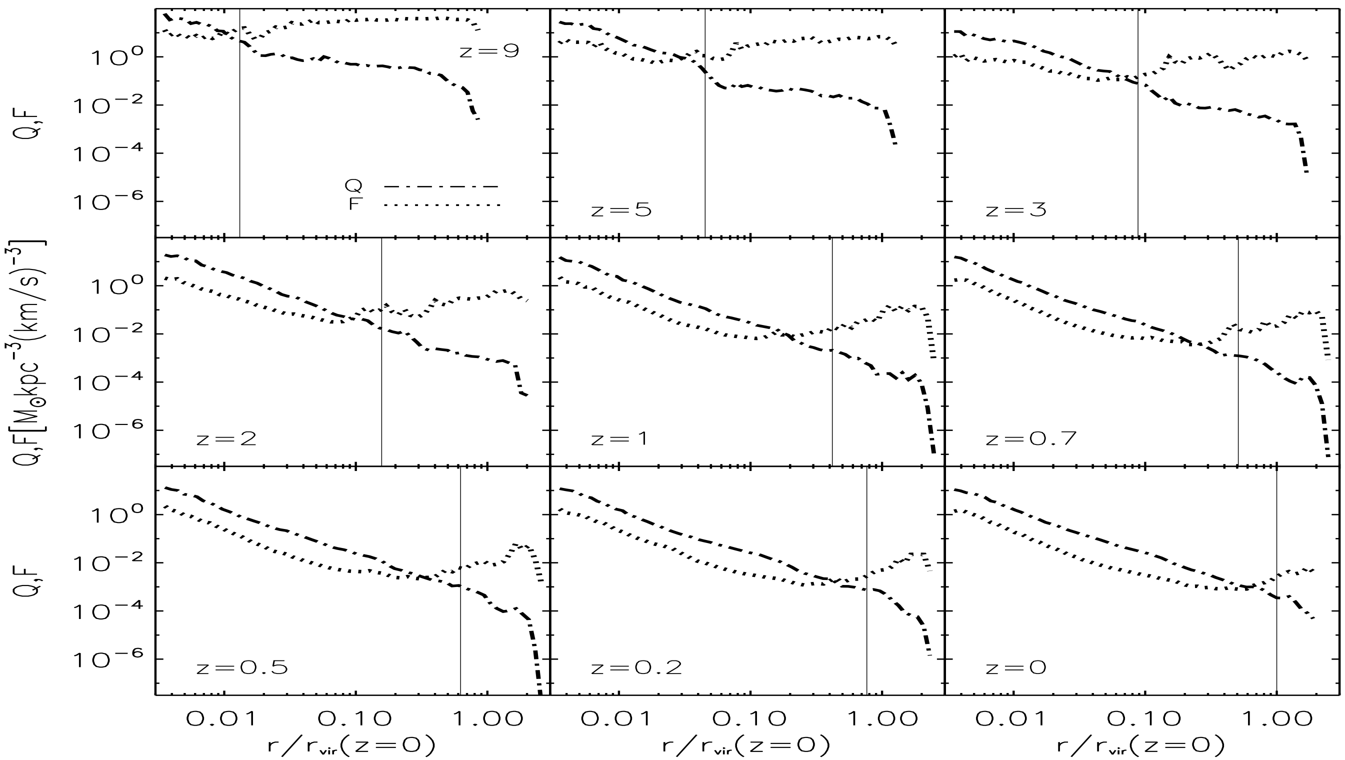

Phase-space density $Q \equiv \rho/\sigma^3$ vs. $r/r_{vir}(z=0)$ dot-dashed line for different redshifts: $0 \leq z \leq 9$.

We see that from $z = 9$ to $z = 0$ the r-average of ρ/σ^3 decreases by a factor $Z \sim 10$.

I. M. Vass et al. MNRAS, 395, 1225 (2009).

The self-gravity decreasing factor Z for spirals.

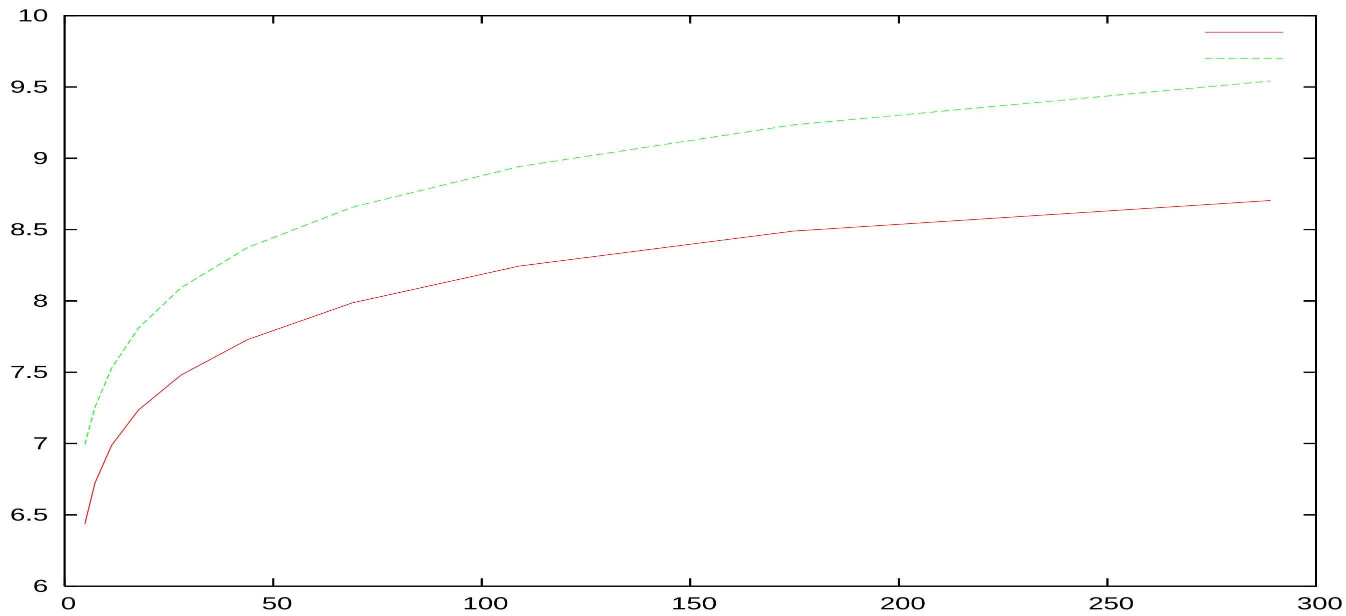

$$Q_{today} = \frac{1}{Z}\, Q_{prim} \quad , \quad Q \equiv \frac{\rho}{\sigma^3}$$

$\log_{10} Z$ in solid red line and the common logarithm of the observed phase-space density $\log_{10} Q_{halo}/(keV^4)$ in broken green line vs. $M_{virial}/[10^{11} M_{solar}]$.

The value of Z depends on the type of galaxy.
Z is larger for spirals than for dSphs.

The observed surface density

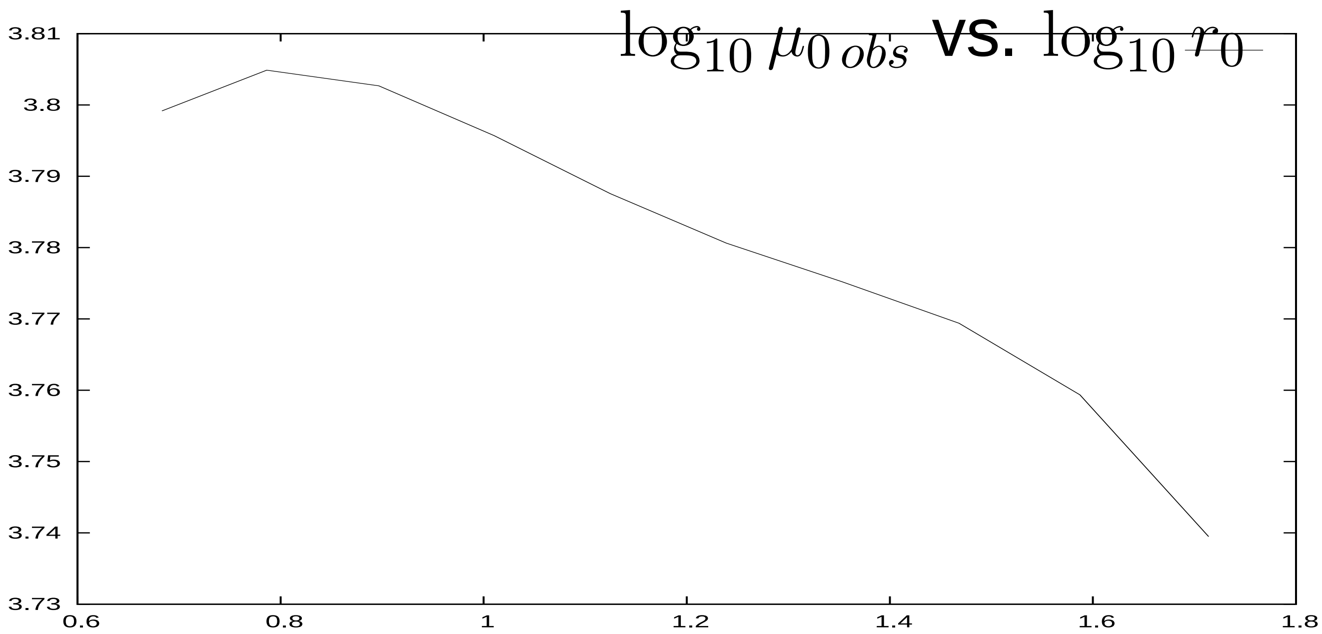

$\log_{10} \mu_{0\,obs}$ in $(\mathrm{MeV})^3$ vs. the common logarithm of the core radius $\log_{10} r_0$ in kpc from spiral galaxies.

Both r_0 and ρ_0 vary by a factor thousand while μ_0 varies only by about $\pm 10\%$.

Relics decoupling non-relativistic

$$F_d^{NR}(p_c) = \frac{2^{\frac{5}{2}}\,\pi^{\frac{7}{2}}}{45}\; g_d\, Y_\infty\; \left(\frac{T_d}{m}\right)^{\frac{3}{2}}\; e^{-\frac{p_c^2}{2\,m\,T_d}} = \frac{2^{\frac{5}{2}}\,\pi^{\frac{7}{2}}}{45}\; \frac{g_d\, Y_\infty}{x^{\frac{3}{2}}}\; e^{-\frac{y^2}{2\,x}}$$

$Y(t) = n(t)/s(t),\; n(t)$ number of DM particles per unit volume, $s(t)$ entropy per unit volume, $x \equiv m/T_d,\; T_d < m$.

$Y_\infty = \frac{1}{\pi}\sqrt{\frac{45}{8}}\,\frac{1}{\sqrt{g_d}\; T_d\; \sigma_0\; M_{Pl}}$ late time limit of Boltzmann.

σ_0: thermally averaged total annihilation cross-section times the velocity.

From our previous general equations for m and g_d:

$m = \frac{45}{4\,\pi^2}\;\frac{\Omega_{DM}\;\rho_c}{g\;T_\gamma^3\;Y_\infty} = \frac{0.748}{g\;Y_\infty}$ eV and $m^{\frac{5}{2}}\;T_d^{\frac{3}{2}} = \frac{45}{2\,\pi^2}\;\frac{1}{g\;g_d\;Y_\infty}\;Z\;\frac{\rho_s}{\sigma_s^3}$

Finally: $\sqrt{m\;T_d} = 1.47\;\left(\frac{Z}{g_d}\right)^{\frac{1}{3}}\;\mathrm{keV}$

We used ρ_{DM} today and the decrease of the phase space density by a factor Z.

Relics decoupling non-relativistic 2

Allowed ranges for m and T_d.

$m > T_d > b$ eV where $b > 1$ or $b \gg 1$ for DM decoupling in the RD era

$$\left(\frac{Z}{g_d}\right)^{\frac{1}{3}} \; 1.47 \text{ keV} < m < \frac{2.16}{b} \text{ MeV } \left(\frac{Z}{g_d}\right)^{\frac{2}{3}}$$

$g_d \simeq 3 \quad \text{for} \quad 1 \text{ eV} < T_d < 100 \text{ keV}$ and $1 < Z < 10^3$

$1.02 \text{ keV} < m < \frac{104}{b} \text{ MeV} \quad , \quad T_d < 10.2$ keV.

Only using ρ_{DM} today (ignoring the phase space density information) gives one equation with three unknowns: $m, \; T_d$ and σ_0,

$\sigma_0 = 0.16 \text{ pbarn } \dfrac{g}{\sqrt{g_d}} \, \dfrac{m}{T_d}$ http://pdg.lbl.gov

WIMPS with $m = 100$ GeV and $T_d = 5$ GeV require $Z \sim 10^{23}$.

Linear results for μ_{0D} and the profile vs. observations

Since the surface density $r_0\, \rho(0)$ should be universal, we can identify $r_{lin}\, \rho_{lin}(0)$ from a spherically symmetric solution of the linearized Boltzmann-Vlasov equation.

The comparison of our theoretical values for μ_{0D} and the observational value indicates that $Z \sim 10 - 1000$. Recalling the DM particle mass:

$m = 0.568 \left(\frac{Z}{g}\right)^{\frac{1}{4}}$ keV for Fermions.

This implies that the DM particle mass is in the keV range.

Remarks:

1) For larger scales nonlinear effects from small k should give the customary r^{-3} tail in the density profile.

2) The linear approximation describe the limit of very large galaxies with typical inner size $r_{lin} \sim 100$ kpc.

Halo radius in the linear approximation vs. observations

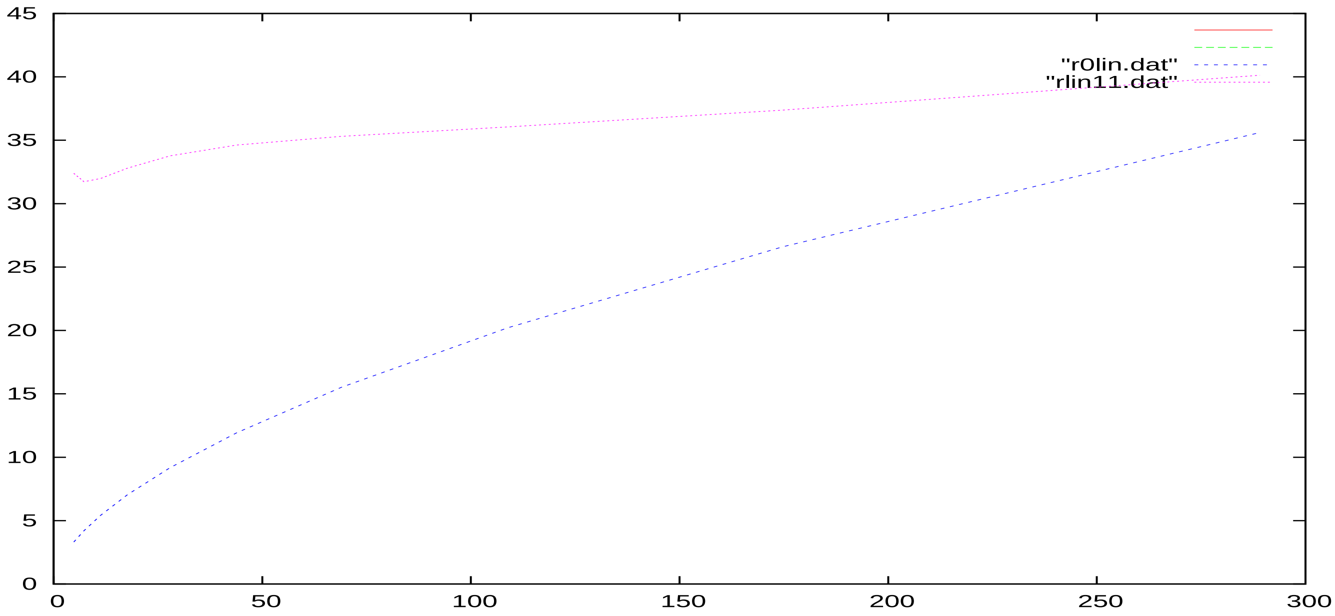

The halo radius in the linear approximation $r_{0\,lin}$ in kpc in broken green line, the halo radius r_0 from the data in kpc in solid red line vs. the galaxy virial mass $M_{virial}/10^{11} M_\odot$.

$$r_{0\,lin} = 52.5 \ \left(\frac{1.8 \text{ keV}}{m}\right)^{\frac{4}{3}} \ \text{kpc}$$

The linear approximation turns to improve for larger galaxies (i. e. more diluted).

Density Contrast

Ratio between the maximum DM mass density $\rho_{lin}(0)$ and the average DM mass density $\bar{\rho}_{DM}$ in the universe

$$\text{contrast} \equiv \frac{\rho_{lin}(0)}{\bar{\rho}_{DM}} = \frac{\mu_{0\,lin}}{\Omega_{DM}\ \rho_c\ r_0}$$

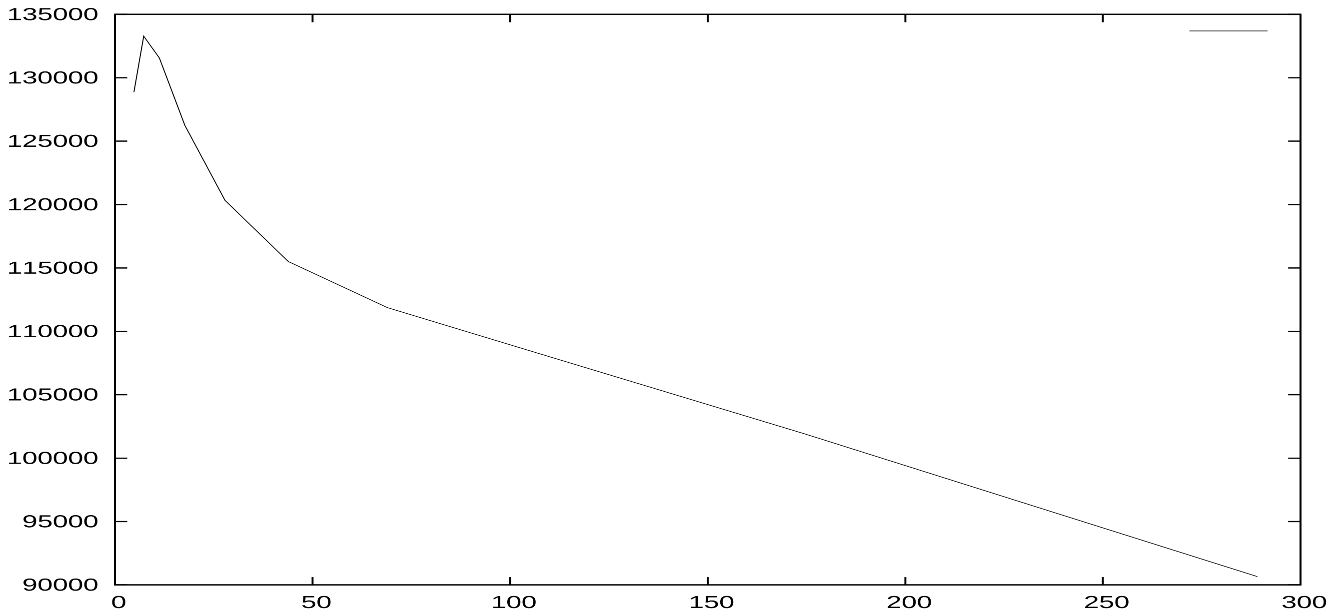

The linear contrast turns to be between 1/3 and 1/2 of the observed value $\sim 3 \times 10^5$ (Salucci & Persic, 1997).

Linear galaxies are less dense and larger than the observations. Universal quantities take the right values.